Iran J Public Health, Vol. 51, No.5, May 2022, pp.1097-1106

Original Article

Phyto-Fabrication of Silver Nanoparticles Using *Typha azerbaijanensis* Aerial Part and Root Extracts

Amir Mirzaie [1], Farzad Badmasti [2], Hedieh Dibah [3], Shadi Hajrasouliha [3], Fatemeh Yousefi [3], Romina Andalibi [4], Aliasghar Bagheri Kashtali [3], Amir Hossein Rezaei [5], *Ronak Bakhtiatri [6]

1. *Department of Biology, Parand Branch, Islamic Azad University, Parand, Iran*
2. *Department of Bacteriology, Pasteur Institute of Iran, Tehran, Iran*
3. *Department of Biology, Roudehen Branch, Islamic Azad University, Roudehen, Iran*
4. *Department of Biology, Medical Science Branch, Islamic Azad University, Tehran, Iran*
5. *Department of Research and Development, Production and Research Complex, Pasteur Institute of Iran, Tehran, Iran*
6. *Department of Pathobiology, School of Public Health, Tehran University of Medical Sciences, Tehran, Iran*

***Corresponding Author:** Email: rbakhtiari@sina.tums.ac.ir

(Received 21 Jul 2021; accepted 12 Oct 2021)

Abstract

Background: Silver nanoparticles (AgNPs) were phyto-synthesized using Typha azerbaijanensis aerial part and root extracts, and their biological activities were investigated.

Methods: This study was conducted in the Science and Research Branch, Islamic Azad University, Tehran, Iran in 2019. In this experimental study, silver nanoparticles (AgNPs) were phyto-synthesized and the physicochemical properties of AgNPs were determined using UV-Vis (UV-Vis) spectroscopy, scanning electron microscopy (SEM), transmission electron microscopy (TEM) and Fourier transform infrared (FTIR) spectroscopy. Antibacterial and anticancer activity of synthesized AgNPs was determined using microdilution assay, and MTT 3- (4,5-dimethylthiazol-2-yl)-2,5-diphenyl tetrazolium bromide) methods, respectively. The apoptotic effects of AgNPs were investigated using Real-Time PCR and flow cytometry techniques.

Results: Morphological analysis of the synthesized AgNPs confirmed the spherical shape of AgNPs with an average size of 10.67 to 16.69 nm. The FTIR spectrum confirmed the presence of phytochemicals from T. azerbayenensis extract at the AgNP surface. Antibacterial experiments showed that phyto-fabricated AgNPs had significant antibacterial activity against Gram-negative bacteria. The AgNPs were significantly cytotoxic against breast cancer cell line (MCF-7) through induction of apoptosis.

Conclusion: The phyto-synthesized AgNPs had biological activities could be useful in pharmaceutical applications.

Keywords: *Typha azerbaijanensis;* Silver nanoparticle; Antibacterial; Anticancer; Antioxidant; Apoptosis

Introduction

Nanotechnology has promising applications in medicine and drug delivery along with cancer treatment and several other fields (1). Metal nanoparticles, especially silver nanoparticles

(AgNP) which have controlled size, shape, and structure have wide applications in medicine (2). In general, there are different physical and chemical methods for synthesizing AgNPs (3-4). However, these methods use different chemical compounds for synthesis that are toxic.

Recently, the phyto-synthesis of AgNP using plant extracts has attracted the attention of researchers. In phyto-synthesis, seeds, gums, fruits, roots, skin, and flowers can be used to synthesize AgNP (5). In addition, the phyto-synthesis of AgNP using plant extracts is cost-effective and environmentally friendly (6). In general, plant extracts contain compounds such as polyphenols, which are secondary compounds that mediate AgNP synthesis (7).

So far, various plant extracts have been used to synthesize AgNP (8-12). In the present study, we used *Typha azerbaijanensis* extract for AgNP synthesis for the first time. *T. azerbaijanensis* is a species of the genus *Typha* that grows in northeastern Iran. The name will not be communicated to the independent Republic of Azerbaijan. The region of Azerbaijan in northeastern Iran may be notified (8-12). These species have different biological properties such as antibacterial, anticancer, antioxidant, anti-diabetic, antiemetic, antihypertensive, hypoglycemic, hypolipidemic effects (13). Phytochemical studies of these species have shown that they are rich in tannins, phenols, flavonoids, carotenoids, and alkaloids, which have been reported to show high antioxidant activities and can be a major factor in reducing silver to AgNP (14).

We performed this study by synthesizing, characterizing, and evaluating the antibacterial, anticancer, and antioxidant potentials of phyto-synthesized AgNPs from aqueous silver nitrate (AgNO3) using aerial parts and root extracts of *T. azerbaijanensis*.

Materials and Methods

Ethical considerations

This study was conducted in the Science and Research Branch, Islamic Azad University, Tehran, Iran in 2019. Ethics approval for this study was obtained from Islamic Azad University, Tehran, Iran permitted this study with number: IR.IAU.REC.1398.029.

Phyto-synthesis of AgNPs

For the synthesis of silver nanoparticles (AgNPs), 4 ml of aqueous and ethanolic extracts of aerial parts and roots of *T. azerbaijanensis* were added to 100 ml of 0.01 mM silver nitrate (AgNO3) (Merck, Germany). After stirring for 45 minutes at room temperature, the solution became colorless brown, indicating reducing of Ag to AgNP. After 45 minutes, the formed precipitate was washed three times with distilled water by centrifugation at 13000 rpm for 20 minutes and the sediment was kept at 60 °C for 2 h (15).

Characterization of AgNPs

UV-Vis analysis of phyto-fabricated AgNPs by spectrophotometer at wavelengths of 200-700 nm was performed to investigate the maximum absorption. Scanning electron microscopy (SEM) and transmission electron microscope (TEM) was used to determine of shape and size of synthesized AgNPs. FTIR spectroscopy was used to identify functional groups involved in AgNP synthesis. FTIR spectra between 4000 cm - 1 and 400 cm - 1 were recorded at a resolution of 4 cm -1 in transmission

Antibacterial activity

Antibacterial activity of phyto-fabricated AgNPs was performed using the micro-broth dilution method to determine minimum inhibitory concentration (MIC) value. Briefly, various concentrations of AgNP including 100, 50, 25, 12.5, 25.2, 3.125, and 1.56 µg/ml were poured into 96-well plates. Subsequently, bacterial suspensions including *Staphylococcus aureus* ATCC 25923, *Bacillus subtilis* ATCC 23857, *Pseudomonas aeruginosa* ATCC 27853, and *Escherichia coli* ATCC 25922 were added to each well at a concentration of 0.5 McFarland. MIC is defined as the lowest inhibitory microbial growth concentration (17).

MTT assay

Cytotoxic effects of AgNPs against breast cancer cell line (MCF-7) was evaluated using MTT (3-(4,5-dimethylthiazol-2-yl)- 2,5-diphenyltetrazole bromide) colorimetric method. Initially, 10^4 cells were seeded in 96-well plates, followed by 96-well plates in a CO_2 incubator at 37 °C for 24 h. Concentrations of 100, 50, 25, 12.5, 6.25, 3.125, 1.56, 0.78, and 0.39 µg/ml from AgNPs were prepared and added to the wells and the plates were incubated for 24 h, then MTT (Sigma Aldrich, Germany) was added to the well and the reaction mixture was kept at 37 °C for 4 h in a 5% CO_2 atmosphere. The MTT dye was then removed and all wells were dissolved using isopropanol. Finally, the absorbance rate of the samples was measured using an ELISA reader at 570 nm (Oraganon Teknika, Netherlands) in which the cell toxicity was calculated using:

% Cell Survival Rate: (absorbance of control cells/ absorbance of treated cells) × 100

and the IC50 value was determined (18).

Apoptotic gene expression analysis

Real-time PCR was used to analyze the expression of apoptotic genes such as *Bax*, *Bcl2*, *caspase-3* (*CASP3*), and caspase-9 (*CASP9*). Initially, MCF-7 cells were treated with IC50 for 24 h, after which total RNAs were extracted from the cell and converted to cDNA using a cDNA synthesis kit (Qiagen, USA). To perform the Real-Time PCR, each cDNA was used as a template in a 20 µl final volume containing 2 µl cDNA, 10 pmol of each primer (Table 1), and 10 µl Power SYBR Green PCR Master Mix (Applied Biosystems) using Bioneer Real-Time PCR equipment (Korea). The GAPDH gene was used as a housekeeping gene to normalize the levels of mRNA expression and the relative expression of *caspase-3, caspase-9, Bax,* and *Bcl2* genes was calculated using the $\Delta\Delta C_T$ method. The primer sequences of target genes, including *caspase-3* and *caspase-9, Bax* and *Bcl-2,* and *GAPDH* (internal control).

Table 1: MIC of different AgNPs against the tested pathogenic bacteria.

Bacteria	MIC of AgNPs synthesized via an ethanolic extract of aerial part (µg/mL)	MIC of AgNPs synthesized via an ethanolic extract of root (µg/mL)	MIC of AgNPs synthesized via an aqueous extract of aerial part (µg/mL)	MIC of AgNPs synthesized via an aqueous extract of root (µg/mL)
Staphylococcus aureus	25±0.0	100±0.0	25±0.0	50 0.0
Bacillus subtilis	12.5±0.0	50±0.0	25±0.0	50±0.0
E. coli	3.125±0.0	25±0.0	12.5±0.0	25±0.0
Pseudomonas aeruginosa	6.25±0.0	12.5±0.0	12.5±0.0	12.5±0.0

Apoptosis/necrosis test

Flow cytometry analysis

To evaluate the apoptosis/necrosis ratio, MCF-7 cells (1×105 cells/well) were first treated with AgNPs (IC50 concentration) for 24 h, and then the cells were treated with Annexin/Propidium Iodide (PI) and Annexin V/Propidium Iodide (PI) (Apoptosis Detection Kit, Roch, Germany), according to the manufacturer's protocol. Finally, the level of necrotic cells/apoptosis was assessed using flow cytometry. Also, untreated MCF-7 cells were used as controls (19).

Statistical analysis

All experiments of this study were done triplicate and the data were expressed as mean±standard deviation (SD). Also, GraphPad Prism software (version 8) was used to analyze the data and one-way analysis of variance (ANOVA) was used using a post hoc test. Note that P <0.05 was considered significant.

Results

After the addition of aqueous and ethanolic aerial parts and root extracts of *T. azerbaijanensis* to AgNO3 solution, the color of the silver nitrate mixture changed from colorless to brown, which is evidence of the synthesis of AgNPs

One of the tests for detecting the synthesis of AgNPs is to check the maximum ultraviolet-visible (UV-Vis) absorption. To, UV-Vis method was used at wavelengths between 200 to 700 nm. The results showed that the maximum adsorption was at 375 nm and the absence of additional peaks indicated the purity of the synthesized AgNPs. Scanning electron microscopy (SEM) and transmission electron microscopy (TEM) were used to determine the shape and size of AgNP. SEM and TEM results showed that the synthesized AgNPs using the ethanolic and aqueous portions and the root extract had a spherical structure, averaging 10.67, 14.75, 15.61, and 16.69 nm, respectively (Fig. 1).

FTIR analysis

To investigate the presence or absence of biological and functional groups of *T. azerbaijanensis* extract on the synthesized AgNPs, FTIR spectral measurements at a resolution of 4 cm-1 were used. Analysis of FTIR results showed the presence of different tensile bonds at different peaks for each of the synthesized AgNPs. In AgNPs synthesized through aqueous root extract, the adsorption peak at 1384 cm-1 corresponds to the amide II group. The absorption peaks at 2881 cm-1 correspond to the tensile vibrational states of the C-H alkane. The peak at 3745 cm-1 represents the polyphenolic group along with the peak at 914 cm-1, which represents the aromatic rings of C-H vibrations. The peaks at 1000-1300 cm-1 were associated with C-O single bond and peaks at 1747 cm-1 represented carbonyl groups (C = O) from polyphenols. The peak at 613 cm1- and 705 cm-1 showed –C≡C–H: C–H bend, while the peak at 914 cm-1 revealed the O–H bend. In AgNPs synthesized via the ethanolic extract of root, absorbance peak at 609 cm-1 indicated C–Br stretch. The peak at 1222 cm-1 represented C–N stretch, while the peak at 1708 cm-1 pointed to C=O stretch. The peak at 2796 cm-1 represented H–C=O: C–H stretch. In AgNPs synthesized via the aqueous extract of the aerial part, the peak at 1060 cm-1 and 1160 cm-1 represented C–N stretch; the peak at 1697 cm-1 and 2892 cm-1 showed C=O stretch and C–H stretch respectively. The peak at 3027 cm-1 represents =C–H stretch, while the peak at 971 cm-1 revealed =C–H bend; the peak at 1180 cm-1 indicated C–N stretch; at 1693 cm-1 represented C=O stretch; at 2935 cm-1 was associated with C–H stretch; the peak at 3341 cm-1 represented the O–H stretch. The pattern of XRD peaks related to the cubic structure of surface centers (fcc) (Face-centered cubic) (111), (200), (220), (311) can be seen in the AgNPs range.

The antimicrobial effects of synthesized AgNPs on Gram-positive bacteria (such as *Staphylococcus aureus* and *Bacillus subtilis*) and two Gram-negative bacteria (*E. coli* and *Pseudomonas aeruginosa*) were studied. AgNPs on Gram-positive bacteria had significant antimicrobial effects compared to Gram-negative bacteria. The MIC results are shown in Table 1. Based on the results, AgNPs synthesized through an ethanolic extract of aerial parts showed a very deep antibacterial activity against Gram-positive and gram-negative bacteria in very low concentrations. The cytotoxicity of different AgNPs prepared against MCF-7 cell line was studied by MTT colorimetric assay with different concentrations of AgNPs. The results showed that AgNPs synthesized via ethanolic aerial extract had the maximum inhibitory effect on MCF-7 cells with IC50 = 7.14 µg/ml compared to other synthesized AgNPs.

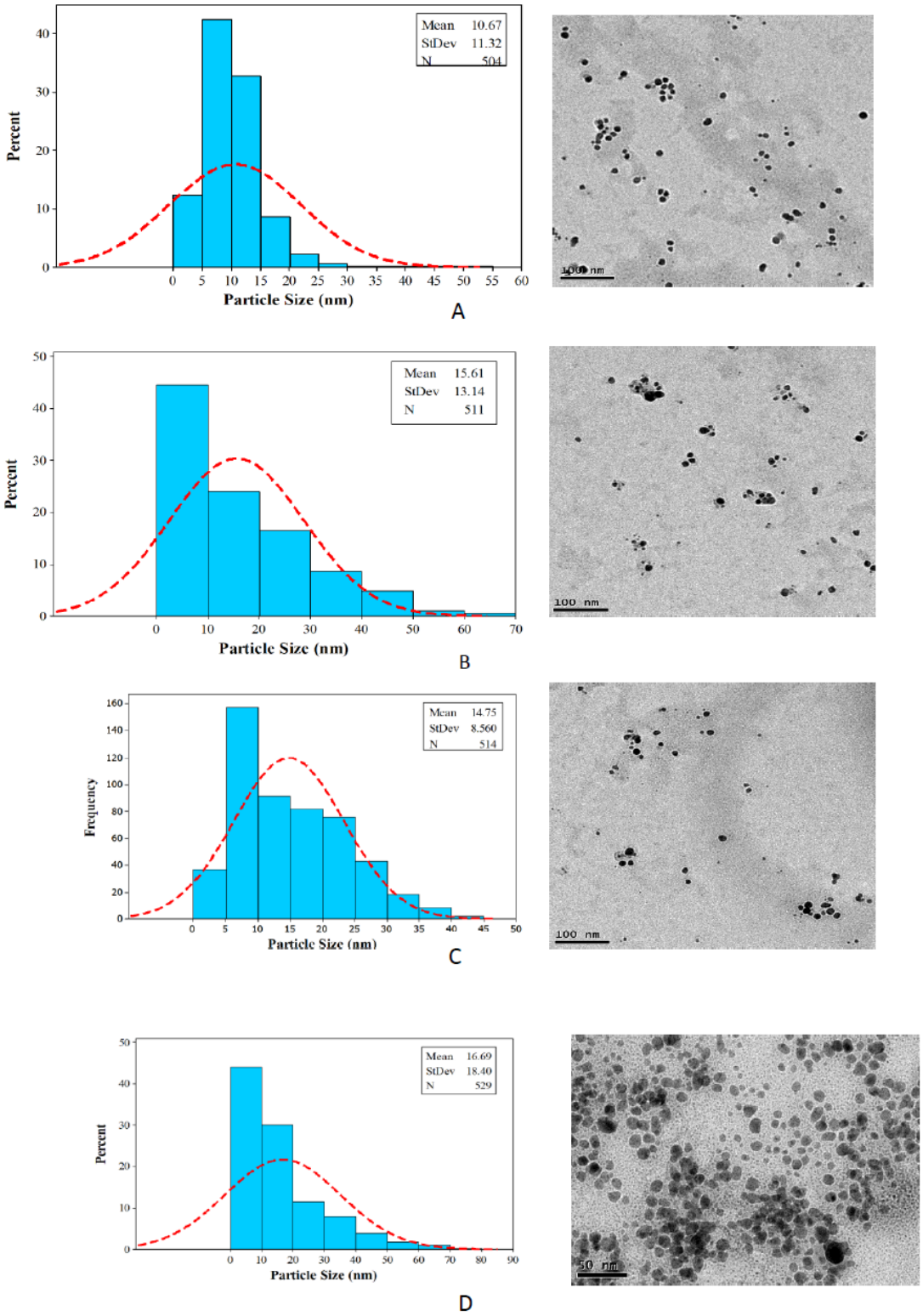

Fig. 1: TEM images of AgNPs synthesized by A: Ethanolic extract of aerial part, B: Ethanolic extract of root, C: Aqueous extract of aerial part, D: Aqueous extract of root

The *Bax, Bcl-2, casp3,* and *casp9* gene expression ratio was assessed in AgNP-treated MCF-7 cells after 24 h. The overexpression of *Bax*, *casp3,* and *casp9* genes (2.91±0.06, 3.29±0.53, and 3.64±0.062, respectively), compared to the reference gene (*GAPDH*), respectively. (0.23±0.049), in the MCF-7 cells treated with AgNPs at 24 h. On the other hand, the expression of *Bcl-2* anti-apoptotic gene was significantly down-regulated in AgNP-treated cells (Fig. 2).

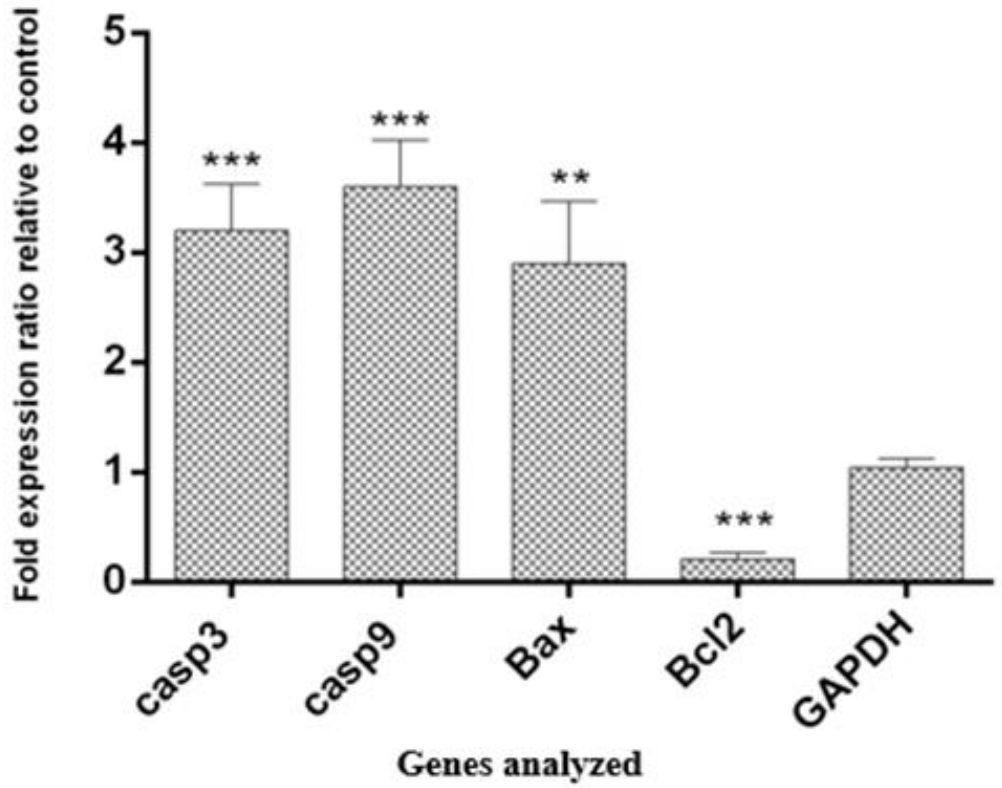

Fig. 2: Comparison of the expression of apoptotic genes in comparison with the reference gene (GAPDH). To evaluate gene expression, MCF-7 cells were treated with silver nanoparticles for 24 hours (*p<0.05, **: p <0.01, *** p <0.001: n=3)

Flow cytometry was used to determine the ratio of apoptosis to necrosis. For this purpose, MCF-7 cells were treated with AgNPs. The cells were stained with FITC Annexin V and PI and analyzed using flow cytometry. Figure 3 shows the flow cytometry results, where the upper left square (Q1) shows the percentage of late apoptotic cells while the upper right square (Q2) shows the percentage of early apoptotic cells. Based on the results, AgNPs synthesized using ethanolic extract of aerial parts resulted in 53.67% primary apoptosis and 7.7% late apoptosis in treated cells.

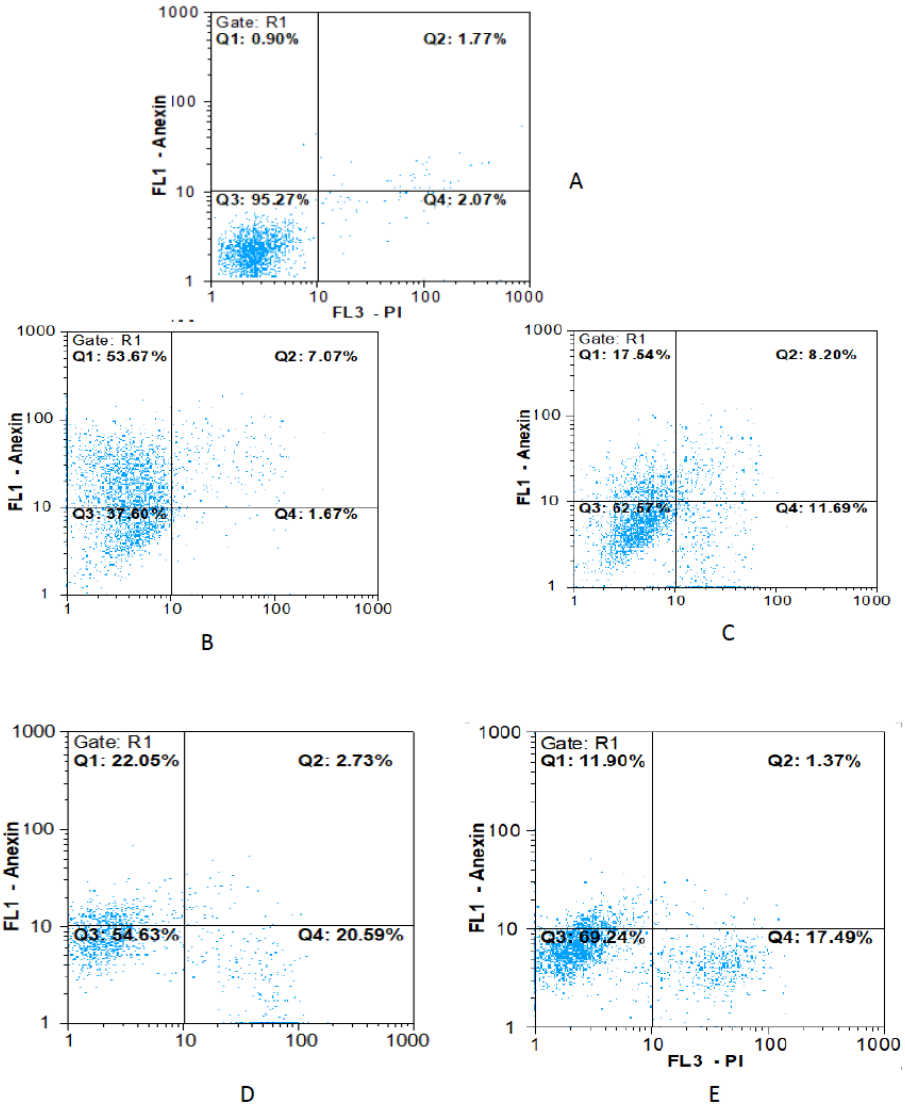

Fig. 3: MCF-7 cell line flow cytometric analysis. A) Un-treated control samples b) samples treated with AgNPs synthesized through aerial ethanolic extract, C: samples treated with AgNP synthesized through ethanolic root extract, D: samples treated with AgNP synthesized via an aqueous extract of aerial parts, E: AgNPs-treated samples are synthesized via aqueous root extract. Lower Left Square: living cells, Upper Left Square: primary apoptosis, Lower Right Square: necrosis, Upper Right Square: delayed apoptosis

Discussion

The bioreduction of AgNO3 is one of the most common methods for the fabrication of AgNPs (20). Among biological methods, phytosynthesis of AgNPs using plant extracts is simple, practicable, sustainable, and cost-effective (21). In the current study, AgNPs were phyto-synthesized using *T. azerbaijanensis* extract and among the extracts, ethanolic extract of aerial parts had high efficiency in the synthesis of AgNPs. To the best of our knowledge, this is the first study to inves-

tigate a simple and rapid method for the fabrication of AgNPs using *T. azerbaycanensisas* extract which acts as a reducing and stabilizing agent and its biological effects were also evaluated. The physicochemical features of the fabricated AgNPs were studied using UV-Vis, FTIR, SEM, and TEM. The UV–Vis spectroscopy measurements of the synthesis of AgNPs via reduction of AgNO3 during the addition of *T. azerbaijanensis* indicated a surface plasmon resonance from the extract at 375 nm. The FTIR analysis of AgNPs synthesized using *T. azerbaijanensis* extract confirmed the capping of synthesized AgNPs by *T. azerbaijanensis* biomolecules. Proteins and enzymes in plant extracts play an important role in the synthesis of AgNPs (22-25). In addition, SEM and TEM analysis showed that the synthesized AgNPs had a spherical shape with an average size between 10.67 and 16.69 nm.

The images also reveal that the AgNPs do not aggregate and are mostly dispersed, thereby confirming the AgNPs-stabilizing nature of the *T. azerbaijanensis* extracts. In addition, the AgNPs synthesized in the current study demonstrated profound antibacterial activity against all tested pathogenic bacteria, while the AgNPs synthesized using ethanolic extract of the aerial parts exhibit effective antibacterial properties. To date, no precise mechanism for the antimicrobial activity of AgNP has been reported. Changes in bacterial membrane morphology increase AgNP permeability and lead to excessive penetration of AgNPs into bacterial cells and eventually, bacterial death occurs (23-26). The secretion of silver ions from AgNP can also enhance the antimicrobial activity of silver nanoparticles (24). Silver ions can bind to oxygen, sulfur, and nitrogen atoms in proteins, resulting in the cessation of cell biochemical reactions and eventual cell death. Bacteria kill bacterial cells (25). In addition, AgNP can alter the structure of cellular DNA by producing toxic oxygen radicals, which eventually, the bacteria will have trouble dividing (25). Based on Sondi and Salopek-Sondi, as well as Gogoi et al., Gram-negative bacteria are more sensitive to AgNP because positive charges of Ag+ with LPS negative charge of the cell membrane in interaction is higher than Gram-positive. Moreover, the morphology and size of AgNP are effective in antimicrobial effects, so spherical nanoparticles have better antimicrobial activity (26). Another objective of this study was to evaluate the antioxidant activity of synthesized AgNPs. Significant anti-DPPH effects confirmed the antioxidant potential of synthesized AgNPs. In this study, AgNPs synthesized by ethanolic extract of the aerial part had a higher antioxidant activity with IC50 = 56.99 µg/ml. The presence of active compounds such as polyphenols, proteins, and alkaloids of plant extracts on AgNP can be one of the reasons for the antioxidant properties of AgNP (27). In addition, we evaluated the cytotoxicity of AgNPs on breast cancer cells (MCF-7) using an MTT assay. AgNP exhibited dose-dependent cytotoxicity against MCF-7 cell cells. Among AgNPs, AgNPs synthesized using ethanolic extract of the aerial part had better cytotoxicity compared to other AgNPs with IC50=7.14 µg/mL. One of the reasons for the better cytotoxicity of AgNPs synthesized from the ethanolic extract of aerial parts compared to others is that it is smaller and then easily passes through the membrane of the cells. Further studies have shown that AgNP is absorbed by mammalian cells through various mechanisms, including phagocytosis, pinocytosis, and endocytosis, and interacts with cellular matter, leading to cell death (28). In the present study, we showed the role of AgNPs in increasing the expression of apoptotic genes, including *Bax, casp 3, casp 9,* and also the *Bcl-2* gene in MCF-7 cells, indicating cellular apoptosis by increasing the permeability of mitochondrial membrane membranes from starts with Bax and Bak proteins. In addition, Bcl-2 and Bcl-xL proteins, which are located at the surface of the endoplasmic reticulum, mitochondria, and mains, prevent the assembly of Bax and Bak proteins and inhibit apoptotic activity (29). In this study, using DAPI staining and DNA fragmentation tests, it was shown that MCF-7 cancer cells undergo DNA fragmentation after treatment with AgNP, which indicates the process of apoptosis. Moreover, the synthesized AgNPs were used to treat cells to assess apoptosis and induce

necrosis. The synthesized AgNPs by the ethanolic extract of an aerial part could induce apoptosis (60%), and had better induction for apoptosis compared to other AgNPs.

Conclusion

Herein, we showed the rapid phyto-fabrication, physico-chemical characterization, and biological activity of silver nanoparticles from various extracts of *T. azerbaijanensis*. The fabrication of AgNPs using *T. azerbaijanensis* extract was a cost-effective and environmentally friendly approach. The synthesized AgNPs showed significant antibacterial, anticancer and antioxidant activity against all tests bacteria, free radicals, and MCF-7 cell line, respectively. In addition, AgNPs had a profound anticancer activity against MCF-7 cells by inducing apoptosis. As a result, AgNPs synthesized from *T. azerbaijanensis* extract could be antibacterial and anticancer agent candidates. Therefore, in the future, with further studies, AgNPs can be used for in-vivo experiments and drug candidate studies.

Journalism Ethics considerations

Ethical issues (Including plagiarism, informed consent, misconduct, data fabrication and/or falsification, double publication and/or submission, redundancy, etc.) have been completely observed by the authors.

Acknowledgements

We hereby thank the Islamic Azad University for providing laboratory facilities for the current study.

Conflict of interest

The authors notify that they have no conflicts of interest.

References

1. Fard NN, Noorbazargan H, Mirzaie A, et al (2018). Biogenic synthesis of AgNPs using *Artemisia oliveriana* extract and their biological activities for an effective treatment of lung cancer. *Artif Cells Nanomed Biotechnol,* 46(sup3):S1047-S1058.
2. Amale FR, Ferdowsian S, Hajrasouliha S, et al (2021). Gold nanoparticles loaded into niosomes: A novel approach for enhanced anti-tumor activity against human ovarian cancer. *Adv Powder Technol*, 32(12):4711-4722.
3. Noorbazargan H, Amintehrani S, Dolatabadi A, Mashayekhi A (2021). Anti-cancer & anti-metastasis properties of bioorganic-capped silver nanoparticles fabricated from *Juniperus chinensis* extract against lung cancer cells. *AMB Express*, 11:61.
4. Ovais M, Khalil AT, Raza A, et al (2016). Green synthesis of silver nanoparticles via plant extracts: beginning a new era in cancer theranostics. *Nanomedicine (Lond),* 11:3157-3177.
5. Behdad R, Pargol M, Mirzaie A, et al (2020). Efflux pump inhibitory activity of biologically synthesized silver nanoparticles against multi-drug-resistant *Acinetobacter baumannii* clinical isolates. *J Basic Microbiol*, 60: 494-507.
6. Ayromlou A, Masoudi S, Mirzaie A (209). *Scorzonera calyculata* aerial part extract mediated synthesis of silver nanoparticles: Evaluation of their antibacterial, antioxidant and anticancer activities. *J Clust Sci*, 30: 1037-1050.
7. Sharma VK, Yngard RA, Lin Y (2009). Silver nanoparticles: green synthesis and their antimicrobial activities. *Adv Colloid Interface Sci*, 145: 83-96.
8. Dehghanizade S, Arasteh J, Mirzaie A (2018). Green synthesis of silver nanoparticles using *Anthemis atropatana* extract: characterization and in vitro biological activities. *Artif Cells Nanomed Biotechnol,* 46(1):160-168.
9. Wintachai P, Paosen S, Yupanqui CT, Voravuthikunchai SP (2019). Silver nanoparticles synthesized with *Eucalyptus critriodora* ethanol leaf extract stimulate antibacterial activity against clinically multidrug-resistant *Acinetobacter baumannii* isolated from pneumonia patients. *Microb Pathog*, 126: 245-257.
10. Arya A, Gupta K, Chundawat TS, Vaya D (2018). Biogenic synthesis of copper and silver nanoparticles using green alga *Botryococcus brauniiand*: its antimicrobial activity. *Bioinorg Chem Appl,* 2018:7879403.

11. Sharma V, Kaushik S, Pandit P, et al (2019). Green synthesis of silver nanoparticles from medicinal plants and evaluation of their antiviral potential against chikungunya virus. *Appl Microbiol Biotechnol*, 103(2):881-891.
12. Iqbal MJ, Ali S, Rashid U, et al (2018). Biosynthesis of silver nanoparticles from leaf extract of *Litchi chinensis* and its dynamic biological impact on microbial cells and human cancer cell lines. *Cell Mol Biol (Noisy-le-grand),* 64(13):42-47.
13. Hamdi SMM, Assadi M (2003). Flora of Iran (Assadi et al.) 42: 13–15, *Typha azerbaijanensis*.
14. Nazemiyeh H, Bahadori F, Delazar A, et al (2008). Antioxidant phenolic compounds from the leaves of *Erica Arborea* (Ericaceae). *Nat Prod Res,* 22:1385-92.
15. Elemike EE, Fayemi OE, Ekennia AC, et al (2017). Silver nanoparticles mediated by *Costus afer* leaf extract: synthesis, antibacterial, antioxidant and electrochemical properties. *Molecules*, 22 (5): 701.
16. Goodarzi V, Zamani H, Bajuli L, Moradshahi A (2014). Evaluation of antioxidant potential and reduction capacity of some plant extracts in silver nanoparticles' synthesis. *Mol Biol Res Commun,* 3(3):165-174.
17. Shadvar P, Mirzaie A, Yazdani S (2022). Fabrication and optimization of amoxicillin-loaded niosomes: An appropriate strategy to increase antimicrobial and anti-biofilm effects against multidrug-resistant strains of *Staphylococcus aureus*. *Drug Dev Ind Pharm*, 1-10.doi: 10.1080/03639045.2022.2027958.
18. Gharaghie TP, Beiranvand A, Riahi A, et al (2022). Fabrication and characterization of thymol-loaded chitosan nanogels: improved antibacterial and anti-biofilm activities with negligible cytotoxicity. *Chem Biodivers*, 19(3):e202100426.
19. Haghighi SM, Tafvizi F, Mirzaie A (2020). Encapsulation of artemisia scoparia extract in chitosan-myristate nanogel with enhanced cytotoxicity and apoptosis against hepatocellular carcinoma cell line (Huh-7). *Ind Crops Prod*, 155:112790.
20. Rasheed T, Bilal M, Li C, Iqbal HMN (2017). Biomedical potentialities of taraxacum officinale-based nanoparticles biosynthesized using methanolic leaf extract. *Curr Pharm Biotechnol,* 18:1116-1123.
21. Ali MA, Mosa KA, El-Keblawy A, Alawadhi H (2019). Exogenous production of silver nanoparticles by *Tephrosia apollinea* living plants under drought stress and their antimicrobial activities. *Nanomaterials (Basel),* 9(12):1716.
22. Rajput S, Kumar D, Agrawal V (2020). Green synthesis of silver nanoparticles using Indian Belladonna extract and their potential antioxidant, anti-inflammatory, anticancer and larvicidal activities. *Plant Cell Rep,* 39(7):921-939.
23. Wu Z, Zhou W, Deng W, et al (2020). Antibacterial and hemostatic thiol-modified chitosan immobilized AgNPs composite sponges. *ACS Appl Mater Interfaces*, 12(18):20307-20320.
24. Targhia AA, Moammeri A, Jamshidifar E, et al (2021). Synergistic effect of curcumin-Cu and curcumin-Ag nanoparticle loaded niosome: Enhanced antibacterial and anti-biofilm activities. *Bioorg Chem*, 115: 105116.
25. Huq MA (2020). Green synthesis of silver nanoparticles using *Pseudoduganella eburnea* MAHUQ-39 and their antimicrobial mechanisms investigation against drug resistant human pathogens. *Int J Mol Sci*, 21(4):1510.
26. Sondi I, Salopek-Sondi B (2004). Silver nanoparticles as antimicrobial agent: a case study on *E. coli* as a model for Gram-negative bacteria. *J Colloid Interface Sci*, 275: 177-82.
27. Docea AO, Calina D, Buga AM, et al (2020). The Effect of silver nanoparticles on antioxidant/Pro-oxidant balance in a murine model. *Int J Mol Sci,* 21(4):1233.
28. Shurpik DN, Sevastyanov DA, Zelenikhin PV, et al (2020). Nanoparticles based on the zwitterionic pillar(5)arene and Ag+: synthesis, self-assembly and cytotoxicity in the human lung cancer cell line A549. *Beilstein J Nanotechnol,* 11:421-431.
29. Bin-Jumah M, Al-Abdan M, Albasher G, Alarifi S (2020). Effects of green silver nanoparticles on apoptosis and oxidative stress in normal and cancerous human hepatic cells in vitro. *Int J Nanomedicine,* 15: 1537-1548.